WATER RESOURCES RESEARCH, VOL. 18, NO. 3, PAGES 645–658, JUNE 1982

Porous Media Equivalents for Networks of Discontinuous Fractures

J. C. S. LONG, J. S. REMER, C. R. WILSON, P. A. WITHERSPOON

Lawrence Berkeley Laboratory, University of California, Berkeley, California 94720

The theory of flow through fractured rock and homogeneous anisotropic porous media is used to determine when a fractured rock behaves as a continuum. A fractured rock can be said to behave like an equivalent porous medium when (1) there is an insignificant change in the value of the equivalent permeability with a small addition or subtraction to the test volume and (2) an equivalent permeability tensor exists which predicts the correct flux when the direction of a constant gradient is changed. Field studies of fracture geometry are reviewed and a realistic, two-dimensional fracture system model is developed. The shape, size, orientation, and location of fractures in an impermeable matrix are random variables in the model. These variables are randomly distributed according to field data currently available in the literature. The fracture system models are subjected to simulated flow tests. The results of the flow tests are plotted as permeability 'ellipses.' The size and shape of these permeability ellipses show that fractured rock does not always behave as a homogeneous, anisotropic porous medium with a symmetric permeability tensor. Fracture systems behave more like porous media when (1) fracture density is increased, (2) apertures are constant rather than distributed, (3) orientations are distributed rather than constant, and (4) larger sample sizes are tested. Preliminary results indicate the use of this new tool, when perfected, will greatly enhance our ability to analyze field data on fractured rock systems. The tool can be used to distinguish between fractured systems which can be treated as porous media and fractured systems which must be treated as a collection of discrete fracture flow paths.

INTRODUCTION

One of the important questions that arises when considering the flow of fluids through a discontinuous rock mass is whether or not the fracture network behaves like a porous medium. In other words, can one model the system by an equivalent permeability tensor and proceed to determine the movement of fluids under the application of known boundary and initial conditions?

Work that has been done to determine the equivalent permeability of fractured rocks from information on fracture geometry (assuming an impermeable matrix) can be classified into two categories. Most of the work that has been done falls into the first category where fractures are assumed to be of infinite extent (continuous or extensive fractures). Very little work has been done in the second category, taking into account the finite or nonextensive nature of fracture size.

Mathematical studies of extensive fracture systems were made by *Snow* [1965]. Snow developed a mathematical expression for the permeability tensor of a single extensive fracture of arbitrary orientation and aperture relative to a fixed coordinate system. He then showed that the permeability tensor for a network of such fractures is formed by adding the respective components of the permeability tensors for each individual fracture.

It can be seen in the field that fractures are clearly of finite dimensions. The fact that fractures are finite means that each fracture can contribute to the permeability of the rock only insofar as it intersects other conducting fractures. In the extreme, an isolated fracture which does not intersect any other fracture effectively contributes nothing to the permeability of the total rock mass. This means that flow in any given fracture is not independent of flow in every other fracture. Thus the permeability of a network of fractures is not simply the sum of the permeabilities of each fracture.

Paper number 2W0254.

Two approaches have been taken to account for the finite nature of real fractures. *Parsons* [1966] and *Caldwell* [1971, 1972] have used analogue models to study finite fractures. *Rocha and Franciss* [1977] have proposed a field method for finding a correction factor to *Snow*'s [1965] analysis. Rocha and Franciss's method is empirical and thus does not account for the hydraulic properties of fractures or for fracture geometry.

A significant result of Parson's work was that doubling the permeability of all fracture elements in the x direction was found to increase the permeability in the y direction. This effect would not be seen in extensive fractures, but with finite fractures the net flow in the y direction must proceed through some fractures oriented in the x direction. Also, for a similar reason, permeability in the x direction was less than doubled. This is a significant property of fracture systems.

In all, very little work has been done to quantify the effect of finite fracture length in combination with other geometric factor such as aperture distribution, fracture location, orientation, and density.

HOMOGENEOUS ANISOTROPIC PERMEABILITY

To determine when a fractured medium behaves as a homogeneous, anisotropic medium, the theory and measurement of homogeneous, anisotropic permeability are briefly reviewed here. The theroy of anisotropic media provides a hydraulic criterion for porous mediumlike behavior. The theory of homogeneity provides statistical and scale effect criteria.

Darcy's law was originally postulated for one-dimensional flow. Since directional properties have no impact on one-dimensional flow, permeability was represented as a single scalar quantity. For three dimensions and an anisotropic medium, *Ferrandon* [1948], *Collins* [1961], and others have proposed that

$$v_i = -\frac{\rho g}{\mu} k_{ij} \frac{\partial \phi}{\partial x_j} \qquad i = 1, 2, 3 \qquad j = 1, 2, 3 \qquad (1)$$

where k_{ij} is symmetric and the matrix can be transformed to a diagonal form by a rotation of coordinate axes.

Experimental evidence supports this theory. Anisotropic porous materials which have been tested do, in fact, behave according to this equation. However, as *Collins* [1961] points out, there is no guarantee that every porous material has an orthogonal permeability tensor.

Day [1974], *Hall* [1956], *Hubbert* [1940, 1956], *Irmay* [1955], and *Gray and O'Neill* [1976] have all tried to derive Darcy's law from first principles. These authors start with the Navier-Stokes equations as applied to the details of flow. Then some form of averaging is applied under a set of assumptions about the nature of the flow regimes. The result is an expression relating the averge gradient to the average flux, i.e., Darcy's law.

The major assumption in each of these analyses is the nature of the relationship between local and average velocities. However, in a random porous medium this relationship can ony be invariant for kinematically similar, steady flow regimes. A flow regime is kinematically similar to another when the magnitude of the velocity in one is a simple multiple of the magnitude of the velocity in the other. The direction of velocity is everywhere the same in kinematically similar regimes. To prove Darcy's law, the full details of the flow system under any arbitary set of boundary conditions must be known. In a general random medium this cannot be done. Therefore the only way to show a given random medium has a symmetric permeability tensor is to actually measure the directional permeability. If the measured directional permeability plots as an ellipsoid as described below, then the medium has a symmetric permeability tensor.

Measurement of Directional Permeability

Darcy's law,

$$v_j = k_{ij}\frac{\partial \phi}{\partial x_i} = K_{ij}J_i \tag{2}$$

can be used to examine the theory of directional permeability measurement. Fundamental to directional permeability measurement is the fact that flow and gradient are not necessarily in the same direction. Only when flow and gradient coincide with one of the principal axes of permeability will flow and gradient be in the same direction. This can be seen from inspection of the above Darcy equation. Thus permeability can be measured either in the direction of flux or in the direction of gradient. These measurements can be used to find the permeability tensor for a homogeneous, anistropic medium.

Marcus and Evanson [1961], *Marcus* [1962], and *Bear* [1972] give the expression for permeability both in the direction of flow and in the direction of gradient. Each author shows how the results of directional permeability measurement can be plotted as ellipsoids. A summary of these analyses is presented here in simplified form.

Under steady flow where the direction of flow is known, permeability in the direction of flux, K_f, is defined by

$$v = -K_f J_i m_i \tag{3}$$

where J_i is the gradient, m_i is a unit vector in the direction of the flux, and v is the flux per unit area. Therefore $J_i m_i$ is the component of the gradient in the direction of the flux (Figure 1). We have

$$1/K_f = -J_i m_i / v \tag{4}$$

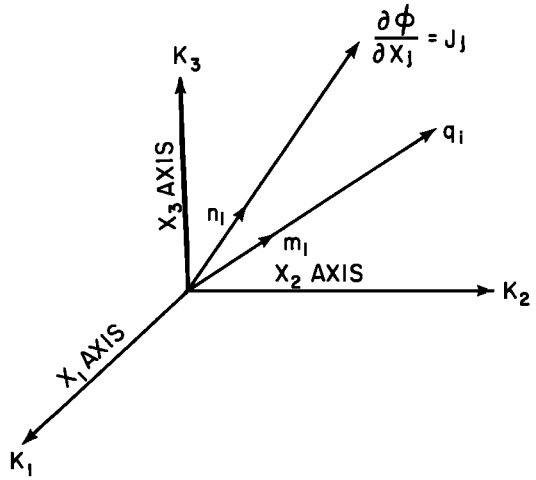

Fig. 1. General flow conditions in anisotropic media.

Substituting Darcy's law,

$$1/K_f = m_i m_j (K_{ji})^{-1} \tag{5}$$

where the components of m_i are the direction cosines of a unit vector in the direction of the flux. If K_f is measured and $\sqrt{K_f}$ is plotted in the direction of m_i, then

$$m_i = x_i/\sqrt{K_f} \tag{6}$$

where the components of x_i give the location of the plotted point. Substituting (6) into (5), we have

$$1 = x_i x_j (K_{ij})^{-1} \tag{7}$$

which is the equation of an ellipsoid with semiaxes of length $\sqrt{K_1}$, $\sqrt{K_2}$, $\sqrt{K_3}$ where K_i, K_2, and K_3 are the principal permeabilities.

Permeability in the direction of the gradient, K_g is defined by

$$v_i n_i = -K_g J \tag{8}$$

where v_i is the flux per unit area, n_i is a unit vector in the direction of the gradient, $v_i n_i$ is the component of flux in the direction of the gradient, and J is the magnitude of the gradient. Substituting Darcy's law, we have

$$K_g = K_{ij} n_j n_i \tag{9}$$

where the components of n_i are the direction cosines of a unit vector in the direction of the gradient. Now if K_g is measured and $1\sqrt{K_g}$ is plotted in the direction of gradient, we have

$$m_i = x_i \frac{1}{\sqrt{K_g}} \tag{10}$$

where the components of x_i give the location of the plotted point. Substituting (10) into (9), we have

$$1 = K_{ij} x_i x_j \tag{11}$$

which is the equation of an ellipsoid with semiaxes of length $1/\sqrt{K_1}$, $1/\sqrt{K_2}$, $1/\sqrt{K_3}$.

For permeability measured in the direction of flux the major axis of the ellipsoid is in the direction of maximum permeability. For permeability measured in the direction of the gradient the major axis of the ellipsoid is in the direction of minimum permeability.

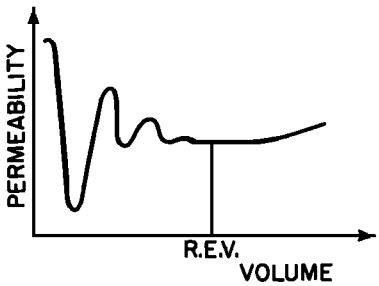

Fig. 2. Statistical definition of a representative elementary volume (REV).

HOMOGENEITY

Another basic problem is that of establishing homogeneity. Homogeneity has been discussed by *Hubbert* [1956], *Fara and Scheidegger* [1961], *Toth* [1967], *Bear* [1972], and *Freeze* [1975]. Freeze points out that there is really no such thing as a truly homogeneous medium in geology. However, in order to have a tractable analysis of flow, a scale of measurement (the macroscopic scale) must be found for which the porous medium is seen as a continuum [*Hubbert*, 1956]. On this scale the medium is said to be homogeneous. The scale at which analysis is possible is commonly illustrated with a diagram such as Figure 2. The volume at which the parameter of interest, in this case permeability, first ceases to vary is defined as the representative elementary volume (REV). Some authors [i.e., *Toth*, 1967] show that as the volume increases still further, the value of the parameter may start to vary again and then become constant again. Thus the 'REV' may exist on several scales. With respect to permeability, the REV of a medium can be sought by measuring the average permeability of increasing volumes of rock until the value does not change significantly with the addition or subtraction of a small volume of rock.

There is no guarantee that such an REV exists for every permeable system. Indeed, *Snow*'s [1969] theoretical and experimental work shows that the permeability of fractured rock may continue to increase with the volume tested. This implies that the statistical sample continues to change with the size of the sample. A further problem has been studied by *Freeze* [1975], *Smith and Freeze* [1979*a*, *b*], and *Smith* [1978]. They have concluded that for some problems it may not always be possible to define equivalent homogeneous properties for inherently heterogeneous systems.

The difficulty in identifying equivalent permeability is that (1) the equivalent permeability tensor that works for one set of boundary conditions may not necessarily predict the correct flux for another set of boundary conditions, and (2) an equivalent permeability which is correct in terms of flux may not predict the correct average head distribution. The first difficulty arises because, in general, different boundary conditions induce different gradients in different parts of the flow field. The permebility is one part of the field which has a higher gradient will have more effect on the total flux than the permeability in another part of the field which has a lower gradient. When the boundary conditions change, the emphasis changes. Therefore a given equivalent permeability tensor will only apply absolutely to kinematically similar flow systems.

If the gradient within the internally heterogeneous REV remains approximately constant, each part of the element will have equal emphasis, and it may be possible to define a unique equivalent permeability tensor which will be correct for linear average flow in any direction. However, if the isopotentials and flow lines are curved relative to the dimensions of the statistically determined REV, then the value of the equivalent permeability of the REV will depend on the particular kinematics of the flow system. In this case, analysis of the flow system would depend on the knowledge of the equivalent permeability, and the value of the equivalent permeability would depend on the flow system. So a unique solution to the flow problem is not guaranteed. Suppose, however, that the gradient is constant and the average flow lines are linear within the statistically determined REV. In this case there may exist a single permeability tensor which can be used to predict correctly flow in any direction. However, even under the constraints of a constant gradient, there is still no guarantee that a unique, symmetric permeability tensor will exist for every medium on any scale.

Given a flow system such as seepage under a dam, the size of the appropriate REV must be small enough to have approximately a constant gradient throughout and therefore linear average flow lines. However, it must also be large enough to contain a representative sample of the heterogeneities. In some cases, it may be that a statistically defined REV is too large to have linear average flow lines. In this case, either a smaller REV must be found as the basis for analysis or a noncontinuum analysis must be used. The size of the relevant REV depends both on the flow system and the medium.

The above discussion leads to several conclusions central to this investigation. First, it only makes sense to look for REV's in fractured rocks using flow systems which would produce a constant gradient and linear flow lines in a truly homogeneous, anisotropic medium. Boundary conditions which produce such a flow system will be described below. Second, the following criteria must be met in order to replace a heterogeneous system of given dimensions with an equivalent homogeneous system for the purposes of analysis:

1. There is an insignificant change in the value of the equivalent permeability with a small addition or subtraction to the test volume.
2. An equivalent symmetric permeability tensor exists which predicts the correct flux when the direction of gradient in a REV is changed.

Point 1 implies that the size of the test volume under consideration provides a good statistical sample of the heterogeneities. Point 2 implies that the boundary conditions are applied to the sample which would produce a constant average gradient throughout a truly homogeneous anisotropic sample. The actual gradient within the heterogeneous sample does not have to be exactly constant for point 2 to be satisfied.

STATISTICS OF FRACTURE GEOMETRY

Under a given set of boundary conditions, the hydraulic behavior of a fractured rock mass with an impermeable matrix is determined entirely by the geometry of the fracture system. Real fractures have complex surfaces and variable apertures, but for the purposes of this study and most other studies of fracture systems, the geometric description is simplified. The assumption is made that individual fractures lie in a single plane and have a constant hydraulic aperture. Characterization of a fracture system is considered complete

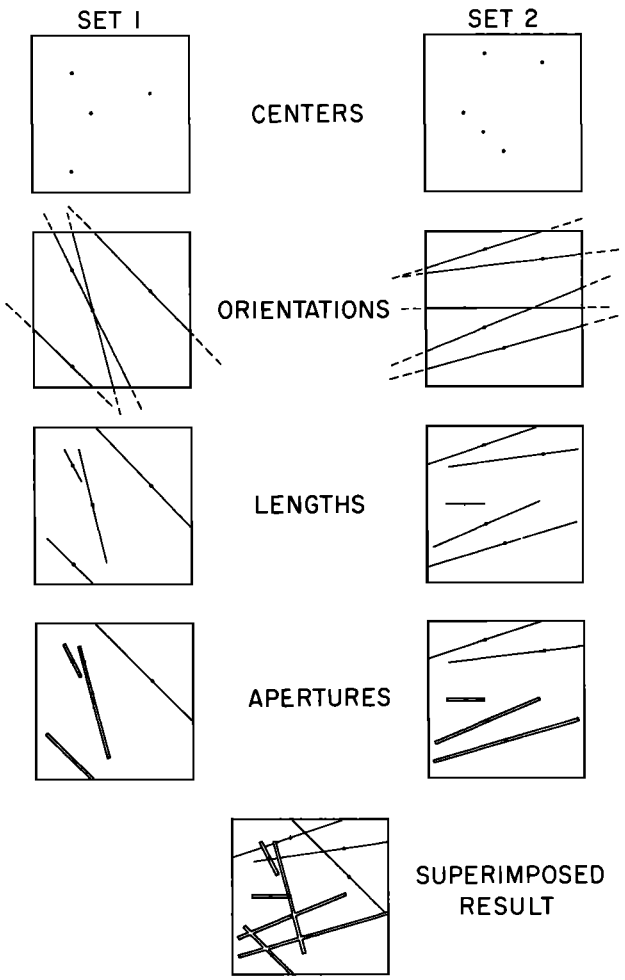

Fig. 3. Superposition of random sets of fractures.

when each fracture is described in terms of (1) hydraulic or effective aperture, (2) orientation, (3) location, and (4) size.

The hydraulic behavior of fractures has been shown to be a function of their effective aperture [*Iwai*, 1976; *Witherspoon et al.*, 1979]. Characterization of the permeability of a fracture requires determining this hydraulic aperture. Unfortunately, it is very difficult to perform hydraulic tests on isolated fractures in the field. For example, *Gale* [1975] isolated a limited number of horizontal fractures with packers and performed injection tests to determine their apertures. Gale's data show poor correlation between hydraulic aperture and observed apparent aperture, but these data are not extensive enough to make significant analysis of the relationship between hydraulic and apparent apertures.

Because of the difficulty involved in hydraulically isolating a single fracture underground, what we know of fracture aperture distributions is limited to apparent apertures that have been observed directly in cores or well logs. The distribution of apertures measured by *Bianchi and Snow* [1968] was found to be very close to log normal. It may be reasonable to expect hydraulic aperture to also be distributed log normally.

The statistics of fracture orientation are perhaps the best understood of all the geometric properties of fractures. Orientation is easily measured in cores or in outcrops with simple tools. For instance, *Mahtab et al.* [1972] developed a computerized method for analyzing clusters of orientation data. Once clusters had been identified, they were compared to Arnold's hemispherical normal distribution.

The mathematical description of fracture locations and fracture dimensions are interrelated. Fracture traces can be observed in outcrops or in excavations. The location of the intersections of fractures with a borehole can also be determined. What we know about the location of fractures in space and their shape and dimensions comes from these trace length and intersection data.

Robertson [1970], *Priest and Hudson* [1976], *Hudson and Priest* [1979], and *Baecher and Lanney* [1978] have studied length and spacing distribution for fractures. *Baecher et al.* [1977] have reviewed this literature on spacing and length distribution. Spacing and length have both been reported to vary exponentially and log normally. *Baecher and Lanney* [1978] developed a conceptual joint geometry model. Joint trace lengths were assumed to be log normally distributed, and spacings were assumed to be exponentially distributed. Beacher and Lanney infer that joints are circular disks randomly distributed in space. Joint radii are shown to be log normally distributed.

Numerical Method of Analysis

A numerical code has been developed to generate sample fracture systems in two dimensions using the geometric properties described above and to determine the permeability of such systems. The computer program has been used to study samples of both extensive and nonextensive fracture networks.

The two-dimensional mesh generator produces random realizations of a population of fractures. Input to the generator includes specification of the distributions that describe the fracture population. The mesh generator can randomly choose fractures for the sample according to these distributions. A finite element analysis can then be used to calculate Q_g, the component of flow through the pattern in the direction of the gradient. Using Darcy's law, the hydraulic conductivity in the direction of the gradient of the sample fracture pattern is calculated from

$$K_g = Q_g/(A\nabla\phi) \tag{12}$$

where A is the gross area perpendicular to flow. The analysis of permeability is independent of the type of fracture model generated. This generator produces models similar to *Baecher and Lanney*'s [1978], but another fracture model, such as that proposed by *Veneziano* [1979], could just as easily have been used.

The effect of sample size on conductivity measurement can be studied with this program. First, a large fracture pattern is generated. A small piece of this sample can be numerically isolated and subjected to the numerical conductivity test described above (equation (12)). Succeedingly larger pieces can be tested and the results compared.

The program can also be used to study the variation in conductivity between different realizations of a statistically described fracture system. This Monte Carlo type analysis could also be used to analyze statistical data collected in the field. An expected value and standard deviation of equivalent porous media conductivity could be obtained in this way.

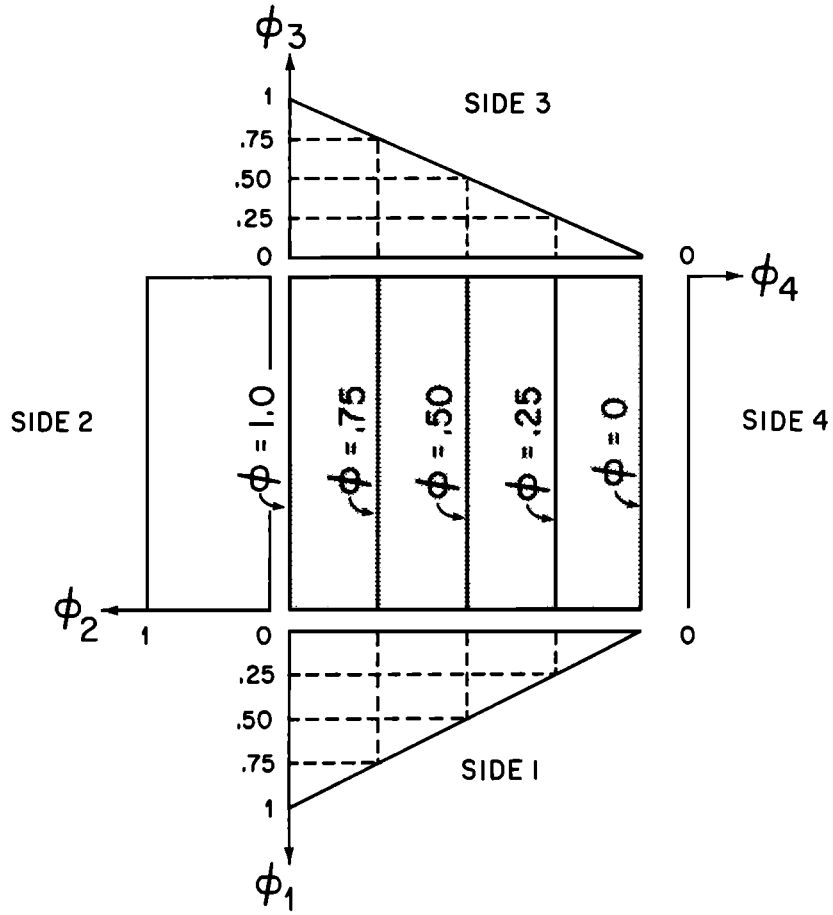

Fig. 4. Boundary conditions applied to fracture models for permeability measurement.

MESH GENERATION

Two-dimensional fracture patterns are produced according to currently available descriptions of real fracture systems. Sets of fractures are assumed to be independent, and individual fractures are randomly located in space. Length distributions are assumed to be log normal or exponential, and apertures are assumed to be log normally distributed. Orientation is normally distributed.

A particular sample fracture pattern is randomly generated in a rectangular or square area (generation region) of any given dimension. A general description of this process follows. Each set of fractures is generated independently. Then the individual sets are superimposed (Figure 3). The location of each fracture in a set is found by assuming that the center of the fractures are randomly distributed (Poisson distribution) within the generation region (Figure 3*a*). For each set a density (number of fractures per unit area) must be supplied to determine the total number of fracture centers to be generated. The orientation of each fracture in a set is determined next (Figure 3*b*). Orientation of fractures in a set has been assumed to be normally distributed. Therefore the mean and variance for orientation must be supplied for each set. At this point the equation of the line on which the fracture lies is identified. The length of each fracture is chosen next (Figure 3*c*). Fracture length within a set is assumed to be distributed log normally or exponentially. The mean and variance for length in the case of a log normal distribution, or the parameter λ, in the case of the exponential distribution, must be supplied for each set. Fracture centers have been constrained to lie within the generation region. However, when lengths are assigned, part of the fracture may be outside the boundaries. These fractures are truncated at the boundaries of the generation region. Finally, apertures are assigned to each fracture under the assumption that apertures are log normally distributed within a set (Figure 3*d*). A mean and variance for aperture must be supplied for each set. When all the sets have been generated, a flow region is selected. The fractures which lie in the flow region are identified, and the coordinates of each intersection are calculated.

MEASUREMENT OF CONDUCTIVITY

As previously discussed, conductivity of a homogeneous medium can be defined either in the direction of flow or in the direction of the gradient. We wish to measure the conductivity of a heterogeneous medium, fractured rock. Gradient can be approximately linear throughout a heterogeneous region in steady flow if the region is an REV. The direction of detailed flow, however, is controlled by the direction of the fractures, and thus the average flow direction is difficult to control. Thus a method which obtains conductivity in the direction of the gradient must be used.

The boundary conditions necessary to produce a linear gradient in a rectangular anisotropic flow region are illustrated in Figure 4. They consist of two constant head boundaries (ϕ_2 and ϕ_4) and two boundaries with the same linear varia-

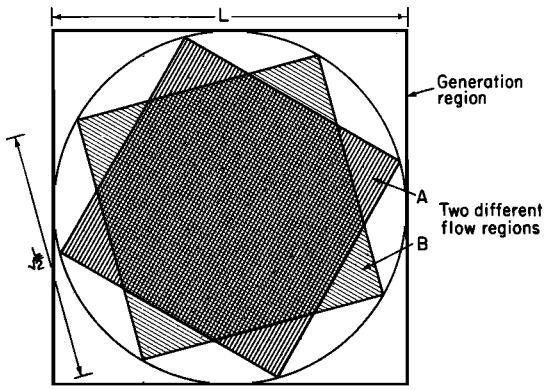

Fig. 5. Two different flow regions within a generation region.

tion in head from $\phi_2 = 1.0$ to $\phi_4 = 0$. An example of the configuration used in these analyses is shown in Figure 4. Conductivity is measured in the direction perpendicular to sides 2 and 4.

The linearly varying boundary conditions on sides 1 and 3 are necessary because, in general, the medium in the flow region is anisotropic. Without these boundaries the lines of constant head would be distorted near sides 2 and 4.

For the boundary conditions shown in Figure 4 in a local x-y coordinate system, $\partial\phi/\partial y$ is zero. $K_g = K_{xx}$ can be calculated:

$$K_g = K_{xx} = Q_x \Big/ \left[\frac{(\phi_2 - \phi_4)L}{L}\right] = Q_x/(\phi_2 - \phi_4) \qquad (13)$$

For $\phi_2 = 1$, $\phi_4 = 0$, and consistent units, K_{xx} is numerically equal to Q_x. Also, since Q_y is also known, K_{xy} can be calculated:

$$K_{xy} = Q_y \Big/ \left[\frac{\phi_2 - \phi_4)L}{L}\right] = Q_y/(\phi_2 - \phi_4) \qquad (14)$$

For $\phi_2 = 1$ and $\phi_4 = 0$, as above, $K_{xy} = Q_y$.

Rotation of the Flow Region

Conductivity in a fracture pattern can be measured in any direction chosen. Figure 5 shows the relationship between the generation regions and the flow regions chosen for analysis. Boundary conditions are applied to the boundaries of this flow region, and conductivity is measured relative to the orientation of the flow region.

In general, the fracture pattern results in an anisotropic medium. For homogeneous anisotropic media, $1/[K_g(\alpha)]^{1/2}$ versus α, the angle of rotation, is an ellipse when plotted in polar coordinates. However, for inhomogeneous fractured media, $1/[K_g(\alpha)]^{1/2}$ may not plot as a smooth ellipse. In fact, the shape of a plot using measured values of $K_{xx}(\alpha)$ for a given test volume of rock may be quite erratic. This plot is used as a test of whether or not the given volume can be approximated as a homogeneous porous medium. If $1/[K_g(\alpha)]^{1/2}$ does not plot at least approximately as an ellipse, then no single symmetric conductivity tensor can be written to describe the medium. If there is no conductivity tensor, then flow through the medium cannot be analyzed by existing continuum techniques.

Fracture Flow Program

Flow through the fracture system is measured using a finite element program developed by *Wilson* [1970] for fracture flow. Fractures are represented as line elements with flux related to aperture by the cubic law. The rock matrix is assumed to be impermeable. Only the steady state flow rate is calculated.

Validation of Numerical Method

The following two examples will illustrate the use of this numerical method of analyzing flow in two-dimensional networks of fractures. The first example is a fracture system of known conductivity which was used to verify the numerical method of permeability measurement. The conductivity of fracture systems with infinitely long fractures is known

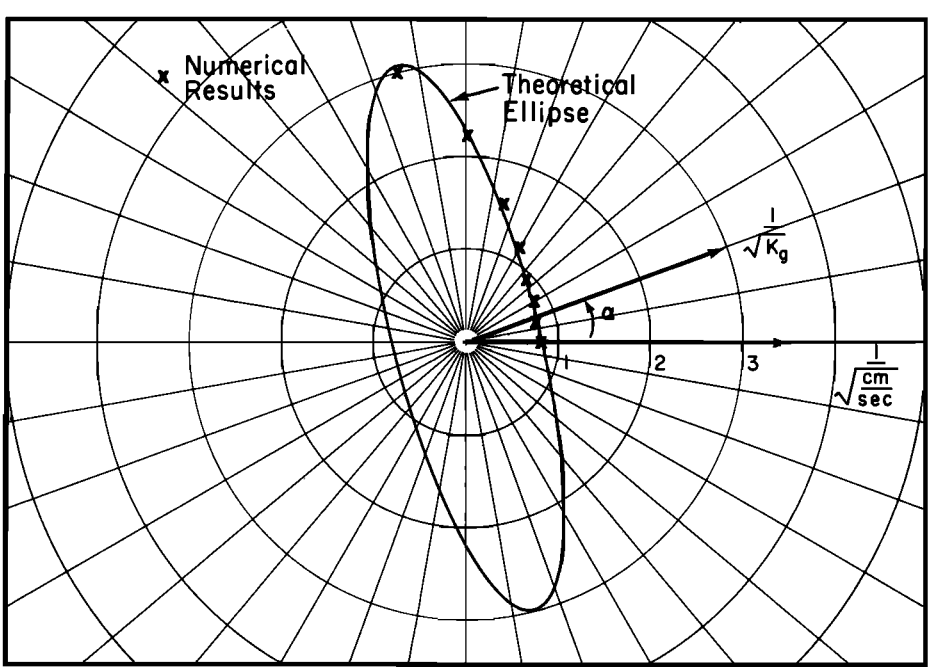

Fig. 6. Comparison between the theoretical permeability ellipse and the numerical results for 'infinite fractures.'

TABLE 1. Input Parameters for Random Network of Fractures

	Parameters	Set 1	Set 2
Density	number of fractures	49	100
Orientation	normal distribution μ, σ^2, deg	30, 5	60, 10
Length	log normal distribution μ, σ^2, cm	40, 10	30, 7.5
Aperture	log normal distribution μ, σ^2, cm	0.001, 0.005	0.005, 0.0001

from the theory developed by *Snow* [1965] and others. Because of the physical basis of this fracture model, we could only examine finite pieces of such fracture systems. The infinite fractures are seen in a finite model as fractures which transect the entire model. An arbitrary extensive fracture system with two sets of parallel, evenly spaced, equal aperture fractures was tested. To provide an anisotropic case, the two sets were placed 30° apart. The numerical code was used to determine K_g for values of α ranging from 0° to 105° as measured from one of the two fracture sets. Theoretically, this fracture network should produce an ellipse for $1/\sqrt{K_g}$, as shown by the solid line on the polar plot in Figure 6. The plotted points represent the results from the numerical analysis as the direction of the hydraulic gradient was changed in increments of 15°. The small differences between theoretical and numerical results can be attributed to the finite nature of the numerical model. Obviously, a fracture network with these properties could be replaced by an equivalent porous medium.

The second example is a nonextensive fracture system that was developed randomly using the mesh generation scheme described above. Table 1 gives the statistics used to generate the fractures. The generation region was 110 × 110 cm.

To determine what variations might be expected from a repetitive generation of networks having the same parameters listed in Table 1, three different fracture systems were examined. Flow regions 75 × 75 cm oriented with $\alpha = 0°$ were investigated in each network. The three regions had network characteristics, as given in Table 2.

Boundary conditions were applied to these three flow regions such that conductivity in the same direction could be measured. That is, sides 1 and 3 were given a linearly varying head distribution, side 2 had a constant head of 1, side 4 had a constant head of zero (see Figure 4). Table 3 gives the total fluxes from each side for each flow region. A positive sign indicates flow into the region, and a negative sign indicates flow out of the region.

Examination of Table 3 leads to several conclusions. First, there is a great deal of variation between the three networks generated using the same statistical fracture population. As shown in Table 2, the number of fractures in each flow region

TABLE 2. Characteristics of Three Random Fracture Networks

Network	Number of Fractures	Number of Fracture Intersections	Number of Nodes	Number of Elements
1	81	123	285	327
2	86	110	282	306
3	90	139	319	368

TABLE 3. Total Fluxes for Three Random Fracture Networks

Network	Side 1, cm^3/s	Side 2, cm^3/s	Side 3, cm^3/s	Side 4, cm^3/s
1	3.13402E-19	4.41796E-7	−4.41384E-7	−4.11388E-10
2	−3.39260E-10	2.00821E-5	−2.00809E-5	−8.67380E-10
3	5.42390E-10	1.01927E-4	−1.01927E-4	−8.97845E-11

varies. Thus some of the variation in flow rate is due to nonergotic sampling. Recall that under the boundary conditions used, for an ideal porous medium the flux in the x direction, i.e., from side 2 to side 4, is numerically equal to the conductivity. However, examination of Table 3 shows that the flux into side 2 does not equal the flux out of side 4. The sum of the fluxes through all sides, however, is zero, as expected. These samples are clearly not behaving like porous media. In anisotropic porous media under the chosen boundary conditions the flux on opposite sides would be equal.

To investigate the problem of directional permeability, network 3 was selected for further analysis. Flow regions 75 × 75 cm in size were rotated at intervals of 15° so that α could be varied from 0° to 180°. Figure 7*a* shows the fracture network of the original generation region and Figures 7*b*–7*d* illustrate how three of the 12 different flow regions were created simply by rotating the boundaries while the network remained fixed.

Figure 8 shows the values of $1/\sqrt{K_g}$ plotted on polar coordinate paper, where K_g is defined in terms of flux across side 2. The fact that inflow does not equal outflow on opposite sides leads to a problem in defining conductivity. If conductivity is arbitrarily defined as numerically equal to the inflow into side 2, no information is lost. Side 2 for any rotation angle α becomes side 4 for $\alpha + 180°$. Therefore, for any rotation angle α, outflow from side 4 equals inflow to side 2 for $\alpha + 180°$.

The results on Figure 8 clearly do not plot as an ellipse nor are they symmetric. For certain angles of rotation (e.g., 75°, 90°) the value of $1/\sqrt{K_g}$ becomes very large and goes off the scale of the graph. For these angles, K_g is very small because there is practically no hydraulic connection between side 2 and any other side. This cannot be completely confirmed visually from the plots of these flow regions because aperture has not been included in the figures. Although average isopotentials have not been plotted for these samples, it is fairly certain they will not be linear.

Similarly, if we define K_{yx} as numerically equal to the flow into or out of side 3, then K_{xy} is the flow into or out of side 1 when the flow mesh is rotated 90°. K_{xy} should equal K_{yx} if K_{ij} is symmetric. For this example, computed values of K_{yx} did not equal computed values of K_{xy} for any angle of rotation. This further demonstrates the nonsymmetric nature of the permeability.

The tests described above show clearly that the sample chosen does not have a symmetric conductivity tensor and cannot be represented by an equivalent porous medium. As further proof of the nonhomogeneous nature of network 3, flow regions of different sizes were extracted and tested. The particular orientation shown on Figure 7*b* for $\alpha = 0°$ was selected, and the flow region was reduced from 75 × 75 cm to 25 × 25 cm, while remaining centrally located in the original generation region. The results revealed order of magnitude changes in hydraulic conductivity from sample to

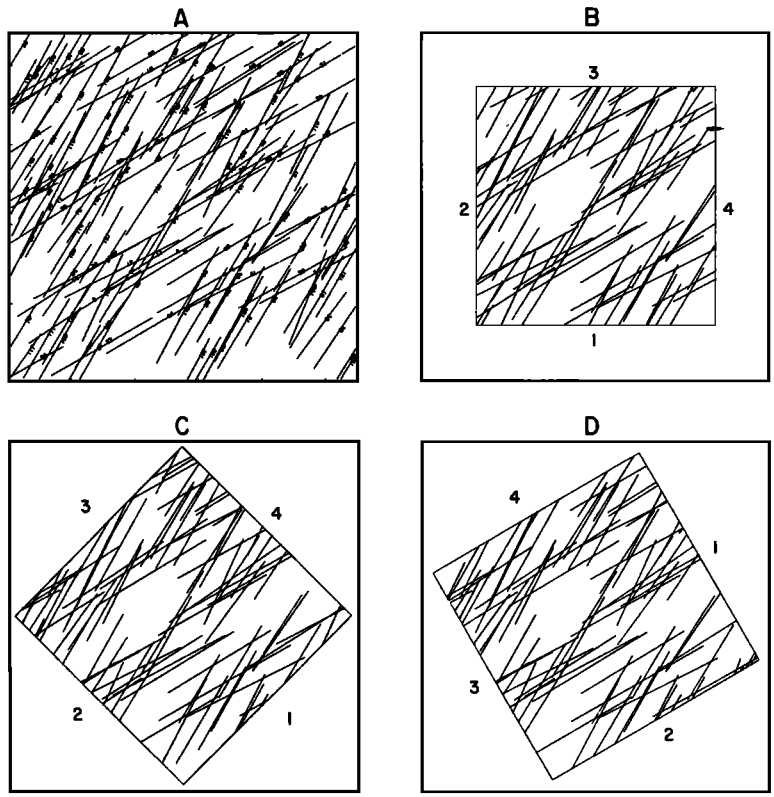

Fig. 7. Generation and three flow regions for random case.

sample and further illustrated the marked differences between the fluid flow behavior of this random fracture network and that of a homogeneous porous medium.

EFFECT OF FRACTURE DENSITY

To see how the density of fractures affected the hydraulic behavior, the following three examples were analyzed. All three examples consisted of two fracture sets with the uniform characteristics given in Table 4. Fracture centers were random as described above.

Figures 9*a*–9*c* show the three fracture meshes studied. The difference between Figures 9*a*, 9*b*, and 9*c* is that the same fractures have been squeezed into successively smaller areas. Figure 9*a* is 40 × 40 cm, Figure 9*b* is 30 × 30 cm, and Figure 9*c* is 25 × 25 cm. Thus the number of fracture

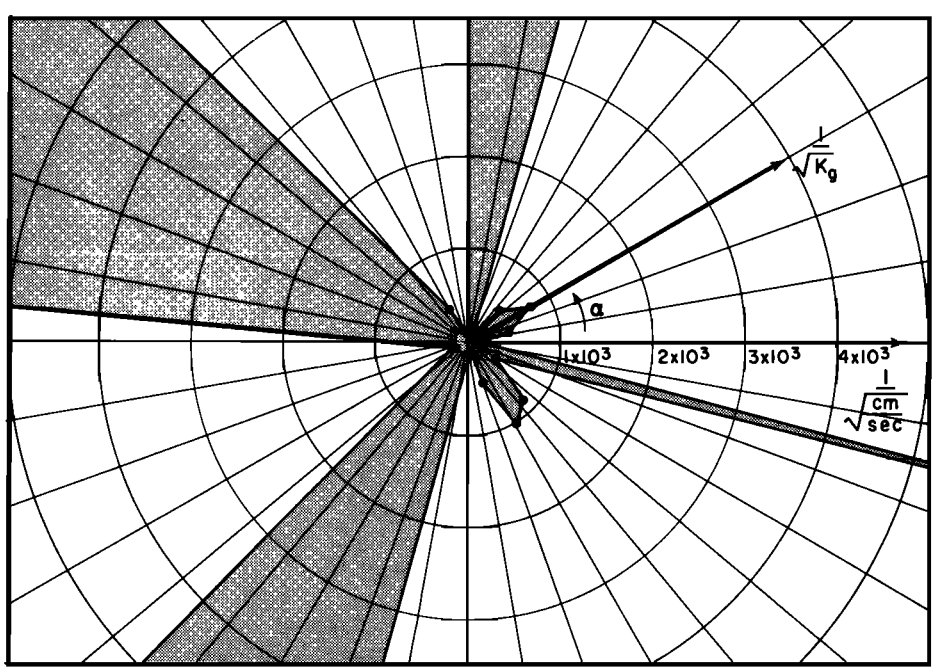

Fig. 8. Values of $1/[K_g(\alpha)]^{1/2}$ plotted on polar coordinate paper.

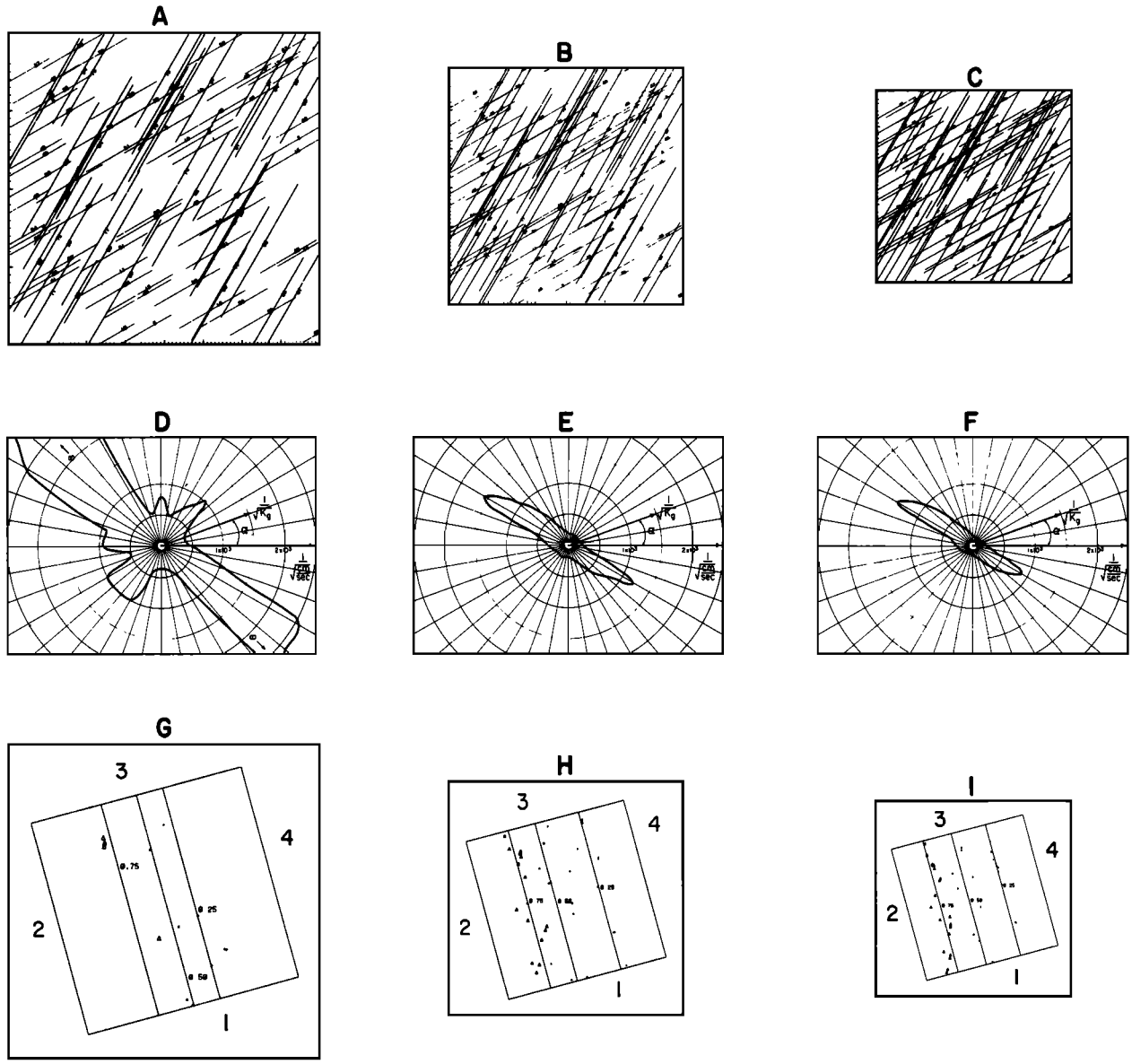

Fig. 9. Fracture systems of increasing density.

intersections and therefore the number of hydraulically active fractures increase. Figures 9*d*–9*f* show the corresponding permeability ellipses for fracture systems of Figures 9*a*, 9*b*, and 9*c*, respectively. The rotated flow regions used to measure permeability in each case were as large as possible.

Comparing the plots from left to right in order of increasing density, there is clearly a significant improvement in the shape of the plots. Figure 9*d* is irregular and nonsymmetric and goes off to infinity for several directions of measurement. Where the plot goes off to infinity the permeability in that direction is zero. This happens for a given direction of measurement when no conducting fractures intersect side 2. For Figure 9*d* this occurred when side 2 was roughly parallel to fracture set 2. It should be noted that a slightly larger or smaller flow region may have eliminated this condition. For Figure 9*e* the fracture density has increased to the point where side 2 always intersects some conducting fractures. Thus no zero permeability directions are found. The ellipse is fairly regular but not symmetric, especially in the direction of minimum principal permeability. Figure 9*f* is slightly improved in this regard. The size of the ellipses decreases from left to right as expected, since denser systems should be more permeable. The direction of minimum and maximum permeability is roughly the same in all three plots.

Figures 9*g*–9*i* show average isopotentials for flow regions at the 15° rotation. For other rotations the plots are similar. The locations on the fractures where heads of 0.75, 0.50, and 0.25 are encountered are plotted on the figures. For a homogeneous porous medium the isopotentials should be equally spaced and all the points should lie on the lines. For

TABLE 4. Fracture System Characteristics for the Density Study

	Uniform Orientation	Uniform Length, cm	Uniform Aperture, cm	Number of Fractures
Set 1	30°	10	0.001	60
Set 2	60°	20	0.002	40

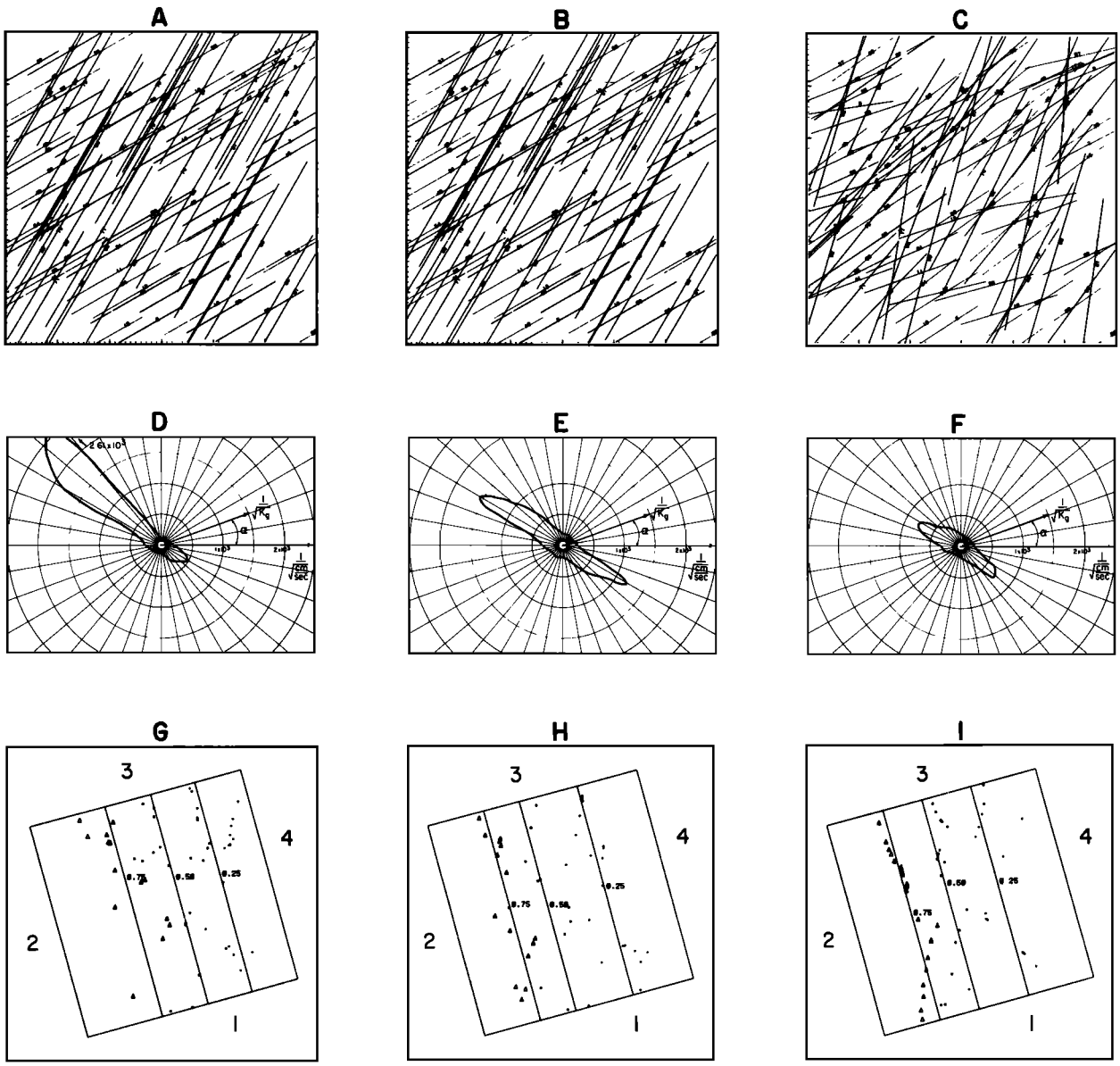

Fig. 10. Fracture systems, with varying parameters.

Figure 9*g*, very few points are plotted because few fractures actually conducted water. In Figure 9*h* the average isopotentials are better spaced. Figure 9*i* shows even more regularity. The scatter of the plotted points also decreases from left to right.

In summary, the hydraulic behavior of the fracture systems becomes more like that of a homogeneous, anisotropic material as fracture density increases. This is an expected result.

Effect of Aperture and Orientation Distribution

The effect of distributing aperture or orientation is illustrated in Figure 10. The fractures shown in Figure 10*b* are exactly the same as the fractures in Figure 9*b*. Consequently, Figures 10*e* and 10*h* are the same as Figures 9*e* and 9*h*, respectively. In Figures 10*a*, 10*d*, and 10*g*, only aperture has been distributed log normally. Figure 10*a* looks exactly like Figure 10*b* because aperture is not shown on the plot. In Figures 10*c*, 10*f*, and 10*i*, only orientation has been distributed normally. All other parameters are uniform.

The permeability plot is skewed for the case where aperture was allowed to vary. In this case, not all the conductors are of equal strength. For some directions of measurement, notably at $\alpha = 135°$, the hydraulic connections to side 2 were evidently through fractures with lower than average aperture. At $\alpha = 30°$, higher than average aperture fractures were intersected by side 2. The flux through a fracture is proportional to aperture cubed. Therefore the measured flux through side 2, which is numerically equal to the permeability, is greatly affected by the size of the fractures intersected by side 2. The fracture meshes in Figures 10*a* and 10*b* have the same number of fracture intersections, but because there is a greater variation in the conductivity of the individual fractures of Figure 10*a*, the results shown in Figure 10*d* are more irregular than the results in Figure 10*e*.

Varying the orientation of the fractures creates hydraulic

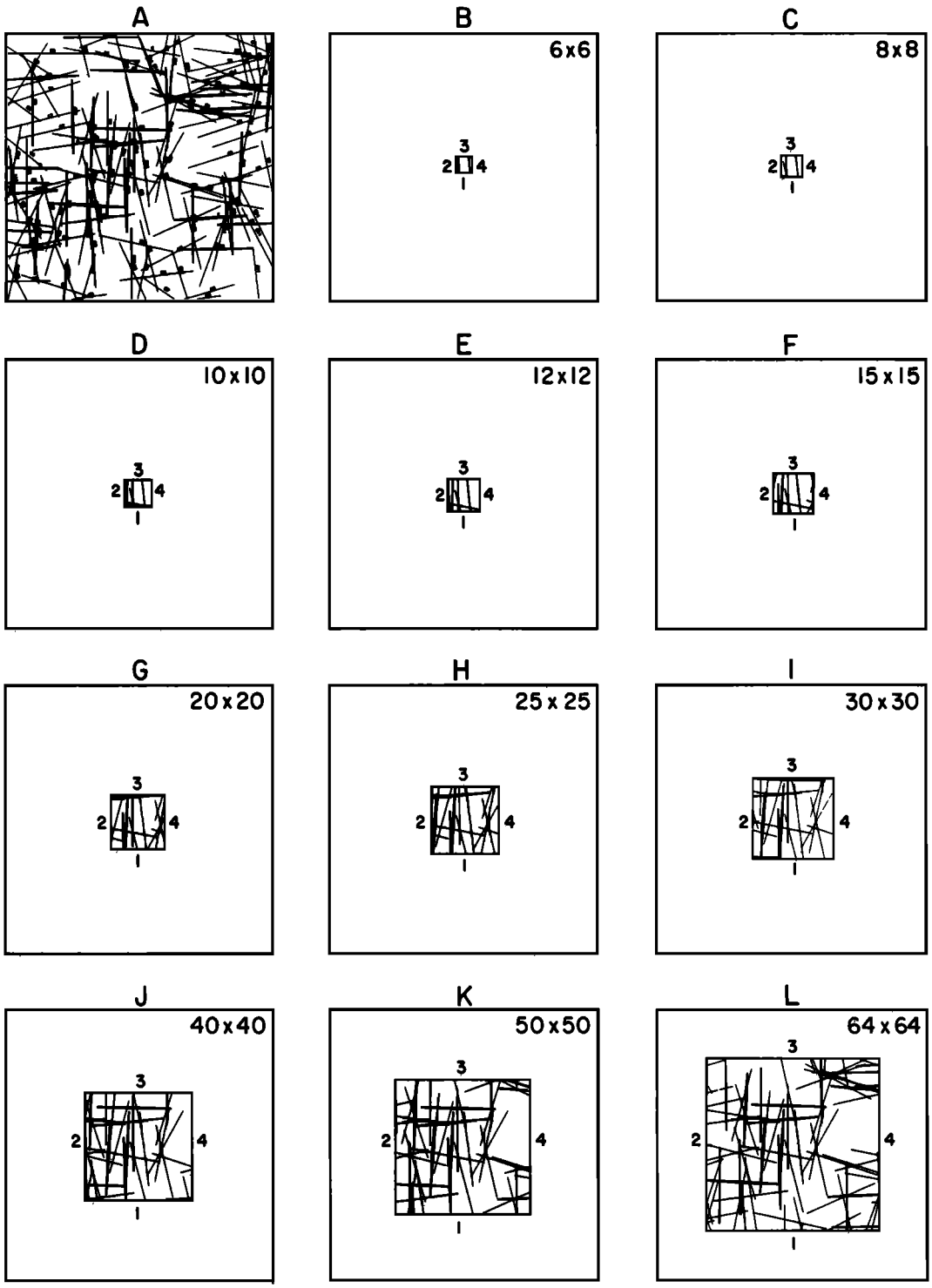

Fig. 11. Fracture samples of increasing size.

behavior more like porous media. In this case the number of fracture intersections increases because fractures of the same set are no longer parallel and now can intersect with each other. The degree of hydraulic connectivity is thus increased and the permeability plot becomes more symmetric and regular. Figures 10*g*–10*i* show slightly improved spacing and decrease in scatter from left to right. Fracture systems with distributed orientations behave more like homogeneous porous media than do systems with uniform orientations. Fracture systems with distributed apertures behave less like homogeneous media than uniform aperture systems.

SCALE EFFECT

The effect of fracture length on the permeability of a fracture system is very sensitive to the scale of measurement. For a scale of measurement smaller than the length of the fracture, the fractures may act as if they were infinite

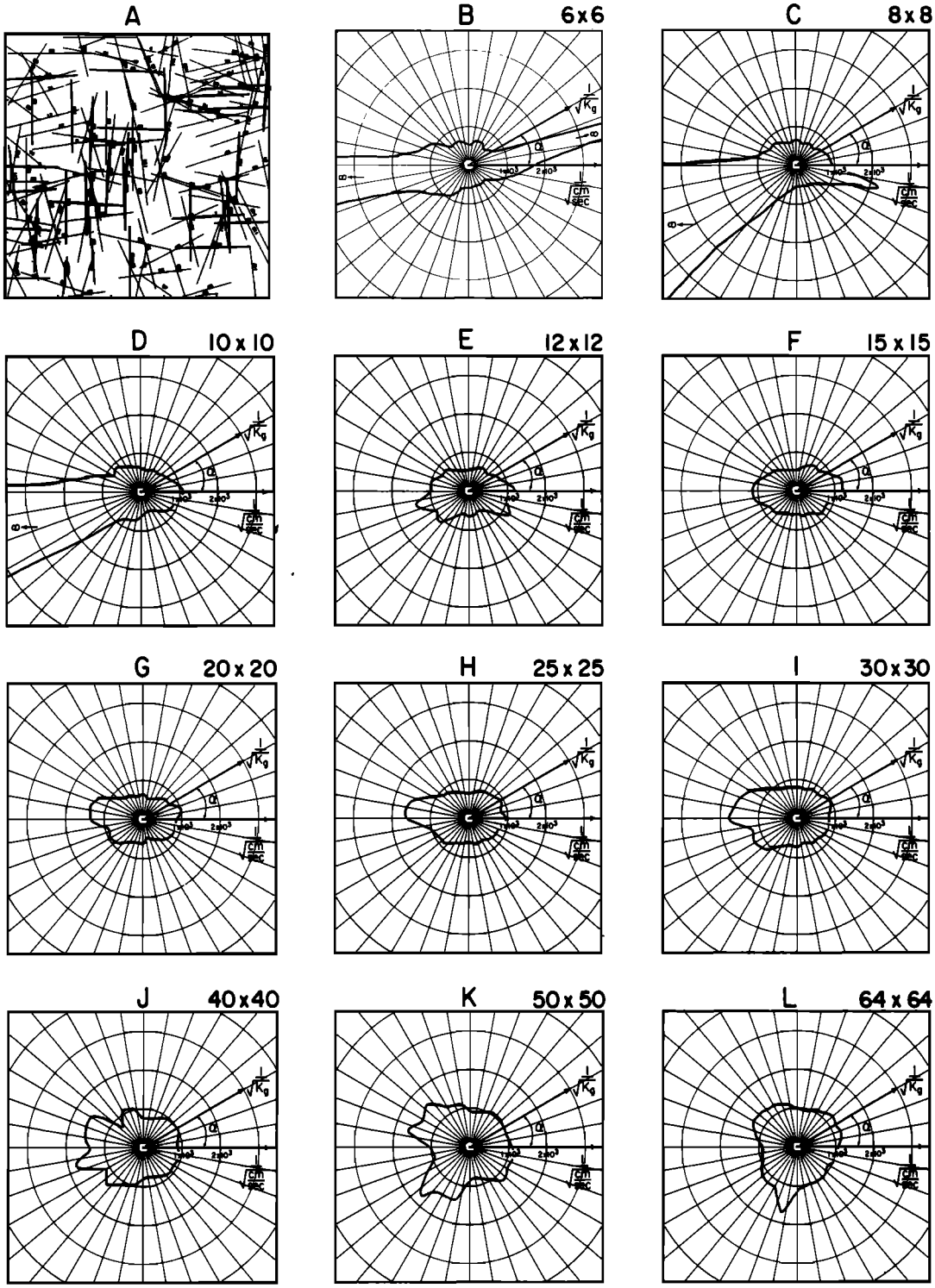

Fig. 12. Permeability plots for fracture samples of increasing size.

relative to the chosen boundaries. At this small scale the fracture system may behave hydraulically like a homogeneous, anisotropic medium. However, as the scale of measurement inceases, the fractures no longer transect the entire measurement volume. The hydraulic behavior of the system may become less regular. In this case only one criterion for equivalent porous medium behavior is met by the small-scale volume. That is, the permeability plots as an ellipse, but the results are still sensitive to volume change.

To illustrate this effect, a system of fractures was chosen with the following properties: The system consisted of two perpendicular sets of fractures all with the same aperture and length. The orientation distribution for each set was the same. The fracture system generated is shown in Figures 11*a* and 12*a*. Theoretically, two orthogonal sets with equal characteristics should have a roughly circular permeability plot. Random variations from the circle can only be due to insufficient density of fractures or insufficient sample size.

Figures 11*b*–11*l* show dimensionless flow regions of increasing size for which permeability measurements were made. These flow regions were all taken from a single generation region 100 × 100 in size. The flow regions are all shown at 0° rotation for illustration. Flow regions at every 15° rotation were used for analysis. Figures 12*b*–12*l* show the corresponding permeability ellipses for the flow regions in Figure 11.

For Figures 12*b*–12*d* the results are erratic. Only a few fractures are included in each sample. In Figure 12*b* only the vertical set is represented and in Figures 12*c* and 12*d* there is only one fracture from the horizontal set. The type of fractures included in the sample is a random function of the location of the flow region. If the flow region had been taken in the upper right-hand corner, the result might have been the opposite with a greater proponderance of horizontal fractures. Although in these three figures most of the fractures transect the flow region, for certain values of the rotation angle, no fractures intersect side 2. Then the permeability is zero, and $1/\sqrt{K}$ is infinite. In Figures 11*e* and 12*e*, enough fractures have been included to provide flow through side 2 for any rotation. In Figure 12*f* for a 15 × 15 mesh a fairly regular symmetric ellipse is obtained. Figure 11*f* shows that for this flow region size many of the fractures transect the entire flow region. However, the ellipse in Figure 12*f* is not circular, as expected. In Figures 12*g*–12*l* the oscillation in the form of the permeability ellipse is due to the increase in sample size. As more fractures are gradually added to the sample, the effect of each fracture is to deform the ellipse in some way. However, the trend from Figures 12*f* to 12*l* is toward the circular ellipse expected.

Although Figure 12*f* shows a seemingly regular ellipse, Figure 11*f* does not include a representative sample of the fracture population. Figure 11*l* is a better sample and Figure 12*l* has a more circular shape. However, Figure 12*l* still shows some perturbations in the hydraulic behavior. The permeability plots may improve somewhat with a further increase in sample size. This can be seen by noticing that there is still a large proportion of truncated fractures in the 64 × 64 mesh. To obtain a good statistical sample of fracture length in the flow region, the flow region should be large compared to the fracture length. In this way a relatively small number of fractures are truncated. Larger samples than 64 × 64 should also be pursued in order to determine if the perturbations in the permeability plot are a function of the sample size or inherent in the facture population. Such an investigation will be possible in the future with a revised configuration of the numerical model.

SUMMARY

For heterogeneous media the REV used in regional groundwater flow problems must be small compared to the size of the flow problem such that each REV experiences a constant gradient. In this way all of the heterogeneities receive the same emphasis.

To test fractured rock samples to see if they behave as porous media, the samples must be subjected to boundary conditions which produce a constant gradient in homogeneous anisotropic media. If the medium has an equivalent porous medium permeability, the tests should have the following results: Directional conductivity measurements $K_g(\alpha)$, using the above boundary conditions should plot as an ellipse when $1/[K_g(\alpha)]^{1/2}$ is plotted versus direction α on polar coordinate paper. Also, inflow will equal outflow on opposite sides of the rectangular volume element tested, and measured values of K_{xy} will equal measured values of K_{yx}. Average gradient should be constant in the element. If the volume of the element tested is changed slightly, the measured value of K_{ij} will not change significantly.

No equivalent homogeneous porous medium permeability will exist for fractured rock populations when the size of REV exceeds the volume of rock that exists or possibly when the fractures are not dense enough to behave as a medium with a symmetric permeability tensor on any scale. In the case of a low density system, the volume of fractured rock may be large enough to be a good statistical sample of the fracture population, but the density of the fractures is such that they will not behave as a porous medium on any scale.

Geometric parameters favoring equivalent porous medium behavior include high density of fractures and nonuniform orientation distribution. A nonuniform aperture distribution detracts from equivalent porous media behavior. The size of an REV may have to be large compared to the fracture lengths in order to provide a good statistical sample of the fracture population.

The techniques described here will be used to direct the emphasis of field testing programs designed to obtain fracture geometry data. Such field tests are currently under development [*Doe and Remer*, 1981]. The numerical model will provide information on the sensitivity of permeability to the individual geometric parameters. In this way, appropriate field tests can be identified. As these field tests are perfected, it will become attractive to extend this model to three dimensions. A three-dimensional model will allow geometric field data to be interpreted in terms of complete permeability tensors.

NOTATION

A	gross area perpendicular to flow, L^2.
b	aperture of a fracture, L.
g	gravitational constant, L/T^2.
J_i	potential gradient = $\partial\phi/\partial x_i$, dimensionless.
K_{ij}, K	hydraulic conductivity, L/T.
K_g, K_f	conductivity in the direction of gradient and flux, respectively, L/T.
k_{ij}, k	intrinsic permeability, L^2
L	length of a fracture, L.
m_i, n_i	unit vectors.
Q	flux, L^3/T.
V	volume, L^3.
v_i, v	flux per unit are (specific discharge), L/T.
x, y	local coordinates, L.
x_i, x_j	global coordinates, L.
δ_{ij}	Kronecker delta, $\delta_{ij} = 1$, if $i = j$, and 0, if $i = j$.
μ	mean value.
μ	viscosity, M/LT.
ρ	density, M/L^3.
σ^2	variance.
ϕ	total hydraulic head, L.
λ	density of fractures (number of fractures per unit area) or exponential distribution parameter.

Acknowledgment. Prepared under U.S. Department of Energy contract W-7405-ENG-48.

REFERENCES

Baecher, G. B., and N. A. Lanney, Trace length biases in joint surveys, *Proc. U.S. Symp. Rock Mech., 19th,* 56–65, 1978.

Baecher, G. B., N. A. Lanney, and H. H. Einstein, Statistical descriptions of rock properties and sampling, *Proc. U.S. Symp. Rock Mech., 18th,* SCI-I–SCI-B, 1977.

Bear, J., *Dynamics of Fluids in Porous Media,* Elsevier, New York, 1972.

Bianchi, L., and D. Snow, Permeability of crystalline rock interpreted from measured orientations and apertures of fractures, *Ann. Arid Zone, 8*(2), 231–245, 1968.

Caldwell, J. A., The theoretical determination of the fluid potential distribution in jointed rocks, M.Sc. thesis, Univ. of Witwatersrand, Johannesburg, South Africa, 1971.

Caldwell, J. A., The theoretical determination of the permeability tensor for jointed rock, paper presented at the Symposium on Percolation Through Fissured Rock, Int. Soc. for Rock Mech. and Int'l Assoc. of Eng. Geol., Stuttgart, 1972.

Collins, R. E., *Flow of Fluids Through Porous Materials,* 275 pp., Reinhold, New York, 1961.

Day, P. R., Soil water dynamics: A syllabus for soil science 220, report, Univ. of Calif., Berkeley, 1974.

Doe, T., and J. Remer, Analysis of constant head well tests in nonporous fractured rock, in *Proceedings of the 3rd Invitational Well-Testing Symposium, Well Testing in Low Permeability Environments,* edited by T. Doe and W. Schwarz, pp. 84–89, Lawrence Berkeley Laboratory, Berkeley, Calif., 1981.

Fara, H. D., and A. E. Scheidegger, Statistical geometry of porous media, *J. Geophys. Res., 66,* 3279–3284, 1961.

Ferrandon, J., Les Iois de L'ecoulement de Filtration, *Genie Civ., 125*(2), 24–28, 1948.

Freeze, R. A., A stochastic-conceptual analysis of one-dimensional groundwater flow in nonuniform homogenous media, *Water Resour. Res., 11*(5), 725–741, 1975.

Gale, J. E., A numerical field and laboratory study of flow in rocks with deformable fractures, 255 pp., Ph.D. dissertation, Univ. of Calif., Berkeley, 1975.

Gray, W. G., and K. O'Neill, On the general equations for flow in porous media and their reduction to Darcy's law, *Water Resour. Res., 12*(2), 148–154, 1976.

Hall, W. A., An analytical derivation of the Darcy equation, *Eos Trans. AGU, 37,* 185–188, 1956.

Hubbert, M. K., The theory of groundwater motion, *J. Geol., 48*(8), 785–944, 1940.

Hubbert, M. K., Darcy's law and the field equations of the flow of underground fluids, *Trans. Am. Inst. Min. Metall. Pet. Eng., 207,* 222–239, 1956.

Hudson, J. A., and S. D. Priest, Discontinuities and rock mass geometry, *Int. J. Rock Mech. Min. Sci. Geomech. Abstr., 16,* 339–362, 1979.

Irmay, S., Flow of liquids through cracked media, *Bull. Res. Counc. Isr., Sect. A, 5*(1), 84, 1955.

Iwai, K., Fundamental studies of fluid flow through a single fracture, Ph.D. dissertation, 208 pp., Univ. of Calif., Berkeley, 1976.

Mahtab, M. A., D. B. Bolstad, J. R. Alldredge, and R. J. Shanley, Analysis of fracture orientations for input to structural models of discontinuous rock, *Rep. Invest. U.S. Bur. Mines, 7669,* 76 pp., 1972.

Marcus, H., The permeability of a sample of an anisotropic porous medium, *J. Geophys. Res., 67,* 5215–5225, 1962.

Marcus, H., and D. E. Evanson, Directional permeability in anisotropic porous media, *Contrib. 31,* 105 pp., Water Resour. Cent., Univ. of Calif., Berkeley, 1961.

Parsons, R. W., Permeability of idealized fractured rock, *Soc. Pet. Eng. J., 10,* 126–136, 1966.

Priest, S. D., and J. Hudson, Discontinuity spacings in rock, *Int. J. Rock Mech. Mining Sci., 13,* 135–148, 1976.

Robertson, A., The interpretation of geological factors for use in slope stability, paper presented at the Symposium on the Theoretical Background to the Planning of Open Pit Mines with Special Reference to Slope Stability, South African Inst. of Mining and Metal., Johonnesburg, 1970,

Rocha, M., and F. Franciss, Determination of permeability in anisotropic rock masses from integral samples, *Structural and Geotechnical Mechanics,* edited by W. J. Hall, pp. 178–202, Prentice-Hall, New York, 1977.

Smith, L., Stochastic analysis of steady state groundwater flow in a bounded domain, Ph.D. dissertation, Univ. of British Columbia, Vancouver, Canada, 1978.

Smith, L., and R. A. Freeze, Stochastic analysis of steady state groundwater in a bounded domain, 1, One-dimensional simulations, *Water Resour. Res., 15*(3), 521–528, 1979*a*.

Smith, L., and R. A. Freeze, Stochastic analysis of steady groundwater flow in a bounded domain, 2, Two-dimensional simulations, *Water Resour. Res., 15*(6), 1543–1559, 1979*b*.

Snow, D. T., A parallel plate model of fractured permeable media, Ph.D. dissertation, 331 pp., Univ. of Calif., Berkeley, 1965.

Snow, D. T., Anisotropic permeability of fractured media, *Water Resour. Res., 5*(6), 1273–1289, 1969.

Toth, J., Groundwater in sedimentary (clastic rocks), paper presented at the National Symposium on Groundwater Hydrology, San Francisco, Calif., Nov. 6–8, 1967.

Veneziano, D., Probabilistic model of joints in rock, report, 47 pp., Civ. Eng. Dep., Mass. Inst. of Technol., Boston, 1979.

Wilson, C., An investigation of laminar flow in fractured porous rocks, Ph.D. dissertation, 178 pp., Univ. of Calif., Berkeley, 1970.

Witherspoon, P. A., J. S. Y. Wang, K. Iwai, and J. E. Gale, Validity of cubic law for fluid flow in a deformable rock fracture, *Water Resour. Res., 16*(6), 1016–1024, 1979.

(Received June 25, 1981;
revised February 4, 1982;
accepted February 12, 1982.)